Astronomy & Astrophysics manuscript no. Irregulares
November 23, 2014

Astrometric positions for 18 irregular satellites of Giant Planets from 22 years of observations

A. R. Gomes-Júnior[1], M. Assafin[1], R. Vieira-Martins[2], J. I. B. Camargo[2]

[1] Observatório do Valongo/UFRJ, Ladeira Pedro Antônio 43, CEP 20.080-090 Rio de Janeiro - RJ, Brazil
e-mail: altair08@astro.ufrj.br
[2] Observatório Nacional/MCT, R. General José Cristino 77, CEP 20921-400 Rio de Janeiro - RJ, Brazil
e-mail: rvm@on.br

Received ; accepted

ABSTRACT

Context. Context
Aims. Aims
Methods. Methods
Results. Results
Conclusions. Conclusion

Key words. Irregular Satellites

1. Introduction

Irregular satellites of the giant planets are smaller than the regular ones with more eccentric, inclined, distant and, in most cases, retrograde orbits. Due to its orbital configurations, it's largely accepted that these objects were captured in the early Solar System (Sheppard & Jewitt 2003).

The majority of these objects was discovery in the last decade [1] mainly because they are faint objects. They were never visited by a spacecraft, with the exception of Phoebe, in a flyby by the Cassini space probe in 2004 (Desmars et al. 2013).

If these objects were captured, there remains the question of where do they come from. Clark et al. 2005 showed from imaging spectroscopy that Phoebe has a surface probably covered by material from the outer solar system.

In this context, we used 3 databases for deriving precise positions for the irregular satellites observed at Observatório do Pico dos Dias (1.6 m and 0.6 m telescopes, IAU code 874), Observatoire Haute-Provence (1.2m telescope, IAU code 511) and ESO (2.2 m telescope, IAU code 809). More than 100 thousand fits images were obtained between 1992 and 2014 covering a few orbital periods of these objects (12 satellites of Jupiter, 4 of Saturn, Sycorax of Uranus and Nereid of Neptune). These positions will be used in new numerical integrations, generating more precise ephemerides. Stellar occultations by these satellites will be better predicted. Once observed, they will make it possible to obtain the satellites' physical parameters (shape, size, albedo, density) with unprecedented precision.

The observations are described in Sect. 2. The astrometric reductions in Sect. 3. The obtained positions are presented in Sect 4 and analysed in Sect. 5. Conclusions are given in Sect. 6.

2. Observations

Our database consisted in optical images from many observational programs performed with different telescopes/detectors targeting a variety of objects, among which irregular satellites. The observations come from 3 sites: Observatório do Pico dos Dias (OPD), Observatoire Haute-Provence (OHP) and European Southern Observatory (ESO). Altogether there are more than 100 thousand FITS images obtained in a large time span (1992-2014). The instruments and images characteristics are described in the following subsections.

2.1. OPD

The first database was produced at Observatório do Pico dos Dias (OPD, IAU code 874)[2], located at geographical longitude $+45^\circ\ 34'\ 57''$, latitude $-22^\circ\ 32'\ 04''$ and an altitude of 1864 m, in Brazil. More than 100 thousand images were observed in 615 nights (244 with Perkin-Elmer, 319 with Boller & Chivens and 52 with Zeiss) between 1992 and 2014 by our group. In Fig 1 there are the quantity of frames obtained by satellite over the time of observations and in Fig 2 the number of frames by satellite for each telescope. Two telescopes of 0.6 m diameter (Zeiss and Boller & Chivens) and one 1.6 m diameter (Perkin-Elmer) were used for the observations.

This is a inhomogeneous database with observations made with 9 different detectors (see Table 1) and 6 different filters. Many of the oldest images headers had missing

Send offprint requests to: A. R. Gomes-Júnior
[1] Website: http://ssd.jpl.nasa.gov/?sat_discovery
[2] Website: http://www.lna.br/opd/opd.html - in Portuguese

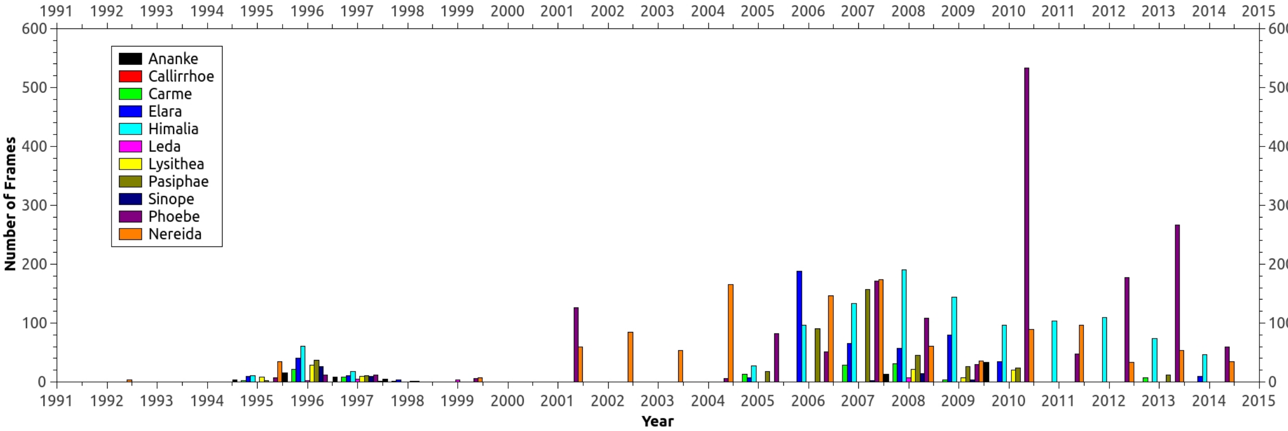

Fig. 1. Distribution of the observations of the satellites over the time from observations at OPD

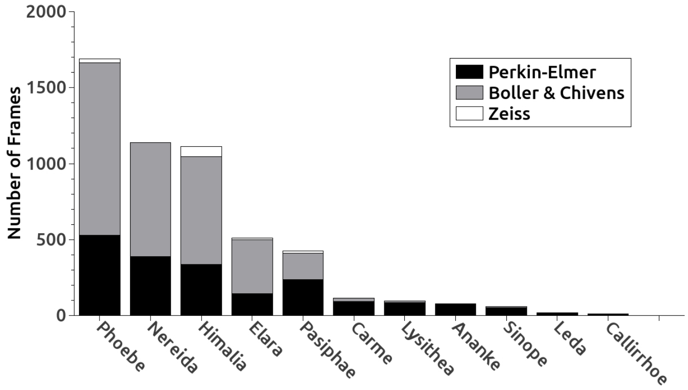

Fig. 2. Number of frames observed by satellite by OPD telescope

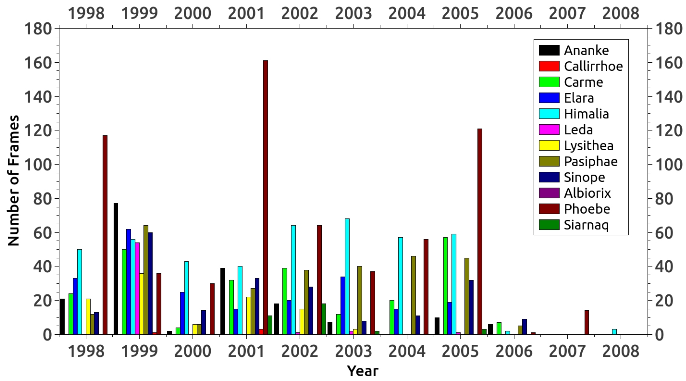

Fig. 3. Distribution of the observations of the satellites over the time from observations at OHP

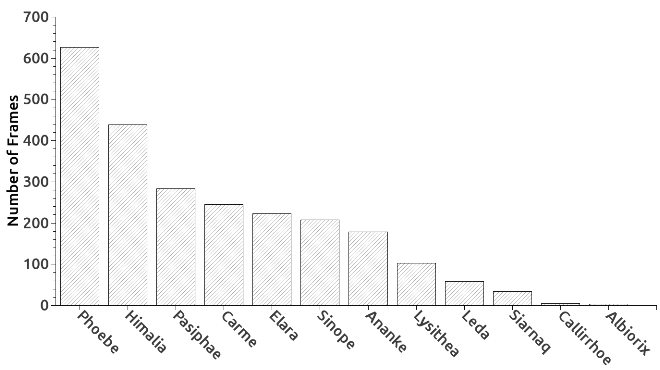

Fig. 4. Number of frames observed by satellite observed at OHP

coordinates or wrong time and in some cases we couldn't identify the detector. The method used to solve this problem will be given in the Sect. 3.

Table 1. Characteristics of OPD detectors used in this work

Detector	Image Size (pixel)	Pixel Size (μm/px)
CCD048	770 x 1152	22.5
CCD098	2048 x 2048	13.5
CCD101	1024 x 1024	24.0
CCD105	2048 x 2048	13.5
CCD106	1024 x 1024	24.0
CCD301	385 x 578	22.0
CCD523	455 x 512	19.0
IKON	2048 x 2048	13.5
IXON	1024 x 1024	13.5

The plate scale of the telescopes are 13.09"/mm for Perkin-Elmer, 25.09"/mm for Boller & Chivens and 27.5"/mm for Zeiss.

2.2. OHP

The instrument used at the Observatoire de Haute Provence (OHP, IAU code 511, 5° 42′ 56.5″ E, 43° 55′ 54.7″N, 633.9 m) was the 1.2m-telescope in a Newton configuration. The focal length is 7.2 m. This database contains more than 20 thousand images obtained in 355 nights between 1997 and 2008. During this time only one CCD detector 1024×1024 was used. The size of field is $12' \times 12'$ with a pixel scale of $0.69''$. All the images were acquired without the use of filters. Fig. 3 shows the Distribution of the observation of the satellites over the time and Fig. 4 the number of frames observed for each satellite.

2.3. ESO

Observations were made at the 2.2 m Max-Planck ESO (ESO2p2) telescope (IAU code 809) with the Wide Field Imager (WFI) CCD mosaic detector. Each mosaic is composed by eight CCDs of $7.5' \times 15'$ (RA, Dec) size, resulting in a total coverage of $30' \times 30'$ per mosaic. Each CCD has $4k \times 2k$ pixel with a pixel scale of $0.238''$. The filter used was a broad-band R filter (ESO#844) with $\lambda_c = 651.725$ nm and $\Delta\lambda = 162.184$ nm. The telescope was shifted between exposures in such a way that each satellite was observed at least twice in different CCDs.

The satellites were observed in 24 nights, divided in 5 missions, between April 2007 and May 2009 during the program that observed stars along the sky path of trans-neptunian objects (TNOs) to identify candidates to stellar occultation as presented in Assafin et al. (2012).

3. Reduction

Almost all the frames were photometrically calibrated with auxiliary bias and flat-field frames by means of standard procedures using IRAF[3] and, for the mosaics, using the esowfi (Jones & Valdes 2000) and mscred (Valdes 1998) packages. Some of the nights at OPD didn't have bias and flat-field images so the correction was not made.

The astrometric reductions were made by the use of the Platform for Reduction of Astronomical Images Automatically (PRAIA) (Assafin et al. 2011). The (x, y) measurements were performed with 2-dimensional circular symmetric Gaussian fits within 1 Full Width Half Maximum (FWHM = seeing). Within 1 FWHM, the image profile is well described by a Gaussian profile, free from the wing distortions, which jeopardize the center determination. PRAIA automatically recognizes catalog stars and determines (α, δ) with a number of models relating the (x, y) measured and (X, Y) standard coordinates projected in the sky tangent plane.

For the ESO images, first the astrometry of the individual CCDs was performed and the (x, y) measurements were corrected by the field distortions patterns determined by Assafin et al. (2012). Finally, all positions coming from different CCds and mosaics were combined to produce a global solution for each night and field observed, and final (α, δ) object positions were obtained in the UCAC4 system.

We used the UCAC4 (Zacharias et al. 2013) as the practical representative of the International Celestial Reference System (ICRS), and the six constants polynomial to model the (x, y) measurements to the (X, Y) tangent plane coordinates. To help identifying the satellites in the frames, and derive the ephemeris for the instants of the observations for comparisons (see Sect 5), we used the kernels from SPICE/JPL[4]. The JPL ephemeris that represented the Jovian satellites was the DE421 + JUP300. For the Saturnian satellites the ephemeris was DE421 + SAT359 to Hyperion, Iapetus and Phoebe and DE421 + SAT361 to Albiorix, Siarnaq and Paaliaq. The DE421 + URA095 was used for Sycorax and DE421 + NEP081 for Nereid.

From Table 2 to 6 there are the mean error in α and δ obtained after these processes by telescope for each satellite. The final number of frames, number of nights and the mean number of UCAC4 stars used in the reduction are also given.

[3] Website: http://iraf.noao.edu/
[4] Website: http://naif.jpl.nasa.gov/naif/toolkit.html

Table 2. Astrometric (α, δ) reduction for each satellite observed with the Perkin-Elmer telescope

Perkin-Elmer					
Satellite	Mean errors σ_α mas	σ_δ mas	Nr frames	Nr nights	UCAC4 stars
Ananke	93.9	185.7	52	7	40
Callirrhoe	66.6	35.4	9	1	3
Carme	97.0	94.3	68	7	49
Elara	230.8	118.7	99	12	32
Himalia	290.5	45.4	238	18	37
Leda	207.4	79.0	6	6	46
Lysithea	107.0	79.4	53	8	41
Pasiphae	157.0	92.5	144	13	22
Sinope	155.0	77.3	37	8	42
Phoebe	73.7	95.3	410	22	6
Nereid	200.3	142.5	289	29	8

Mean errors are the standard deviations in the (O−C) residuals from (α, δ) reductions with the UCAC4 catalog.

Table 3. Astrometric (α, δ) reduction for each satellite observed with the Boller & Chivens telescope

Boller & Chivens					
Satellite	Mean errors σ_α mas	σ_δ mas	Nr frames	Nr nights	UCAC4 stars
Carme	68.5	111.4	22	4	45
Elara	55.4	43.0	294	23	53
Himalia	83.2	43.2	560	31	57
Lysithea	23.6	42.7	7	2	60
Pasiphae	128.5	71.1	140	14	57
Sinope	59.7	17.3	4	1	22
Phoebe	43.8	48.4	810	42	17
Nereid	61.0	45.6	514	38	20

Mean errors are the standard deviations in the (O−C) residuals from (α, δ) reductions with the UCAC4 catalog.

Table 4. Astrometric (α, δ) reduction for each satellite observed with the Zeiss telescope

Zeiss					
Satellite	Mean errors σ_α mas	σ_δ mas	Nr frames	Nr nights	UCAC4 stars
Elara	17.5	21.4	10	1	146
Himalia	112.4	72.3	56	4	91
Pasiphae	24.6	25.1	11	1	140
Phoebe	37.2	30.6	19	1	16

Mean errors are the standard deviations in the (O−C) residuals from (α, δ) reductions with the UCAC4 catalog.

4. Satellite Positions

5. Comparison with current ephemeris

6. Conclusions

Acknowledgements.

Table 5. Astrometric (α, δ) reduction for each satellite observed with the OHP telescope

OHP					
Satellite	Mean errors σ_α mas	σ_δ mas	Nr frames	Nr nights	UCAC4 stars
Ananke	100.6	89.0	141	20	62
Carme	114.9	96.3	204	29	39
Elara	52.0	61.2	187	25	37
Himalia	49.6	66.6	357	43	49
Leda	118.8	33.1	48	7	14
Lysithea	63.0	50.8	84	13	56
Pasiphae	101.0	75.9	248	32	39
Sinope	196.1	73.4	169	25	43
Albiorix	179.0	188.5	4	1	40
Phoebe	30.5	31.9	516	63	51
Siarnaq	46.5	98.4	20	6	32

Mean errors are the standard deviations in the (O−C) residuals from (α, δ) reductions with the UCAC4 catalog.

Table 6. Astrometric (α, δ) reduction for each satellite observed with the ESO telescope

ESO					
Satellite	Mean errors σ_α mas	σ_δ mas	Nr frames	Nr nights	UCAC4 stars
Ananke	225.4	19.1	57	3	761
Callirrhoe	44.6	43.1	20	1	493
Carme	140.4	110.8	37	4	1074
Elara	112.2	87.9	46	4	1492
Himalia	76.7	74.1	23	2	1153
Leda	60.3	125.5	44	3	632
Lysithea	76.4	88.4	90	6	695
Megaclite	52.7	34.9	10	1	445
Pasiphae	70.6	114.8	66	5	836
Praxidike	7.8	38.2	2	1	1934
Sinope	339.1	70.2	11	2	1542
Themisto	894.1	28.5	16	2	1232
Albiorix	76.0	50.9	46	6	330
Paaliaq	301.4	59.0	11	4	382
Phoebe	102.1	57.9	32	5	312
Siarnaq	86.2	66.3	56	6	283
Sycorax	150.7	82.2	35	9	375
Nereid	115.4	78.5	99	12	362

Mean errors are the standard deviations in the (O−C) residuals from (α, δ) reductions with the UCAC4 catalog.

References

Assafin, M., Camargo, J. I. B., Vieira Martins, R., et al. 2012, Astronomy and Astrophysics, 541, A142

Assafin, M., Vieira Martins, R., Camargo, J. I. B., et al. 2011, in Gaia follow-up network for the solar system objects : Gaia FUN-SSO workshop proceedings, held at IMCCE -Paris Observatory, France, November 29 - December 1, 2010. ISBN 2-910015-63-7, ed. P. Tanga & W. Thuillot, 85–88

Clark, R. N. et al. 2005, Nature, 435, 66

Desmars, J. et al. 2013, Astronomy and Astrophysics, 553

Jones, H. & Valdes, F. 2000, in "Handling ESO WFI Data With IRAF", ESO Document number 2p2-MAN-ESO-22200-00002

Sheppard, S. S. & Jewitt, D. C. 2003, Nature, 423, 261

Valdes, F. G. 1998, in "The IRAF Mosaic Data Reduction Package" in Astronomical Data Analysis Software and Systems VII, A.S.P. Conference Ser., Vol 145, eds R. Albrecht, R. N. Hook and H. A. Bushouse, 53

Zacharias, N., Finch, C. T., Girard, T. M., et al. 2013, AJ, 145, 44